An Experimental Study on Heat Transfer Characteristics with Turbulent Swirling Flow Using Uniform Heat Flux in a Cylindrical Annuli

Tae-Hyun Chang*
Division of Mechanical and Automation Engineering, Kyungnam University, 449 Wolyoung Dong, Masan, Kyungnam 631-701, Korea
Kwon-Soo Lee
Department of Mechanical Engineering, Kyungnam University Graduate School, 449 Wolyoung Dong, Masan, Kyungnam 631-701, Korea

An experimental study was performed to investigate heat transfer characteristics of turbulent swirling flow in an axisymmetric annuli. The static pressure, the local flow temperature, and the wall temperature with decaying swirl were measured by using tangential inlet conditions and the friction factor and the local Nusselt number were calculated for Re=30000~70000. The local Nusselt number was compared with that obtained from the Dittus-Boelter equation with swirl and without swirl. The results showed that the swirl enhances the heat transfer at the inlet and the outlet of the test tube.

Key Words : Bulk Temperature, Uniform Heat Flux, Dittus-Boelter Equation, Multi-pitot Tube, Swirl Intensity, Tangential Inlet Condition

Nomenclature

A : Cross section area of the test tube (m^2)
c_p : Specific heat at constant pressure(kJ/kgK)
D : (d_o-d_i) (mm)
d_o : Annulus concave diameter (mm)
d_i : Annulus convex diameter (mm)
f : Friction factor for fully-developed flow
f_s : Friction factor for swirling flow
h : Heat ransfer coefficient (W/m^2K)
k : Thermal conductivity (kW/mK)
L : Length of the swril chamber (m)
Nu : Nusselt number
Nu_s : Nusselt number for swirling flow
P : Fluid pressure (Pa)
P_0 : Atmosperic pressure (Pa)
P_r : Prandtl number
P_s : Static pressure (Pa)
P_v : Total pressure (Pa)
Re : Reynolds number, $\frac{UD}{\nu}$
R_i : Reynolds of the convex tube (mm)
R_o : Radius of the concave tube (mm)
T : Local air temperature (℃)
T_i : Wall temperature on the convex tube (℃)
T_r : Room air temperature (℃)
T_w : Wall temperature (℃)
U : Averaged axial velocity (m/s)
X : Axial coordinates (mm)
y : Radial position (mm)

Greek Letters

ρ : Density (kg/m^3)
v : Kinetic viscosity (m^2/s)
τ_w : Wall shear stress (N/m^2)
θ : Swirl angle (°)

* Corresponding Author,
E-mail : changtae@kyungnam.ac.kr
TEL : +82-55-249-2613; **FAX** : +82-55-249-2617
Division of Mechanical and Automation Engineering, Kyungnam University, 449 Wolyoung Dong, Masan, Kyungnam 631-701, Korea. (Manuscript **Received** November 16, 2002; **Revised** September 25, 2003)

1. Introduction

The flow in a cylindrical annuli, which has

been widely utilized in the boiler feed water heater, heat exchanger between sea water and cooling water, tubular type heat exchangers, cyclotron separator, and rotor cooler, and stator of motor and generator, has been much studied.

One of the first to attempt in the study of this field was Rothfus (1948), who considered the friction coefficient and velocity profiles of air flow in the tube. Next year, he formulated concepts on turbulent intensity and the Reynolds stress. Using a Pitot tube and hot wire anemometer, Bringhton et al.(1964) investigated the mean velocity, turbulent intensity, and Reynolds stress of water in the range of Re=46000 to 327000.

Alan(1967) measured the friction coefficient and velocity profile of water flow in Re=6000 to 9000 through the tube for the ratio of R_o/R_i= 2.88 to 9.37. Other important works on turbulent flow with heat transfer were carried out by Kay et al. in 1963.

Additionally, Tuft et al.(1982) investigated the Nusselt number of water flow through a cylindrical annuli in Re=41~465 by the finite differ ence and experimental methods, and Molki et al.(1990) measured the Nusselt number of air flow through an inner helical convex tube in Re=500~1250 by the naphthalene sublimation method. In the beginning of the 21st century, Garimella et al.(1995) reported that they investigated the tube friction coefficient of water for Re=310~1000 in a scroll annuli with a groove and also the Nusselts number by making use of the LMTD(Log Mean Temperature Difference) method. The tube friction coefficient of the turbulent flow was 10 times greater than that of laminar flow and the Nusselts number was 4~20 times greater than that of the flow.

In the early investigations into the influence of swirl on fluid flow, Chigier et al.(1964), Scott et al.(1973), Milar (1979), and Clayton et al.(1985) studied about the swirl flow through a cylindrical annuli by measuring velocity profiles and pressure losses and applied the numerical analysis method.

Recently, Chang et al.(2001) measured the velocity profiles and Reynolds stress in the horizontal cylindrical tube by using the Particle Image Velocimetry method. Other significant works on turbulent flow were carried out by Kim et al. and Ahn et al.(1993, 1994, 1995, 1999), who found that the surface roughness improved the efficiency of the overall heat transfer after investigating the characteristics of the turbulent flow mechanism and heat transfer in a rectangular annuli of Pr=0.72.

These studies, however, were not clear on how the fluid was heated along the test tube. Furthermore, only few papers have dealt with the description of the local temperature distribution and outer wall temperature in fluid flow in an annuli. Moreover, there is no data for the region where the Nusselts numbers are not fully developed.

The heat transfer coefficient of several heat exchangers has been increased by enlarging the area of heat transfer, introducing artificial illuminators and coils or by protruding fins or making grooves in the tube.

Thus, this study was performed to investigate the characteristics of swirl flow with heat transfer in the horizontal annuli having a radius ratio of R_o/R_i=3.0, to measure the static pressure, the local flow temperature and the tube wall temper ature of swirl and non-swirl flow of Re=30000~ 80000 under a uniform heat flux, and to find out the Nusselts number and contribute to the compact and economical design of heat exchangers.

2. Experimental Apparatus for Heat Transfer

Fig. 1 shows the layout of the experimental apparatus used in this study with swirl and without swirl.

A concave tube, with an inner diameter of 150 mm, and a length of 3000 mm, and a copper tube, with the outer part uniformly wound at the space of 12 mm with a heating coil (Pyrotenax Ltd.) of 2.6 kW, 240 V, were fabricated to uniformly transfer heat to the fluid. The entrance flange of the test tube was made of bakelite, but the exit flange, taking thermal expansion into consideration, was made of Teflon. Sixty-four thermocouples were installed at a space of 90° in

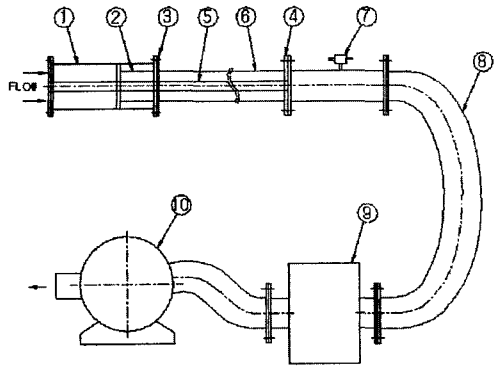

① Swirl chamber	② Swirl generator
③ Teflon flange(for concave tube)	④ Teflon flange (for convex tube)
⑤ Convex tube (PVC tube)	⑥ Test tube (Concave, Copper)
⑦ Multi Pitot tube (TORBAR 301)	⑧ Flexible hose
⑨ Air chamber(ϕ600×H1000mm)	⑩ Suction fan(220V, 10HP)

Fig. 1 Experimental Apparatus for Heat Transfer

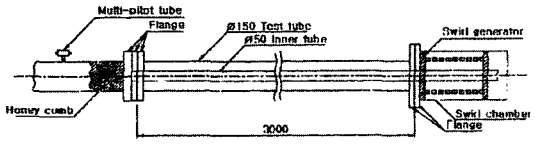

Fig. 2 Schematic Diagram of the Test Tube

16 test tube sections, that is, four thermocouples in a section. In order to measure the inside flow temperature of the test tube, 16 thermocouple ports were installed onto the surface of the test tube, which was wrapped with a glass wool blanket of more than 50 mm thickness.

A voltage regulator was manufactured to adjust the requirement of a 240 V heating coil. A transformer was prepared to measure voltage and current to find heat flux value. Meanwhile, a multi-Pitot tube was installed at the end of tube to identify the Reynolds number of air, from which the fluid velocity was to be determined. The rpm of the fan motor was controlled. The local flow and wall temperature of the tube were measured by thermocouples to determine the heat applied to the fluid.

The swirling generator was fabricated by using an acryl tube with an outer diameter of 166.0 mm. The tube was drilled, with holes having a diameter 3.2 mm at a space of 45° from the outer to inner tangential direction in eight locations. To

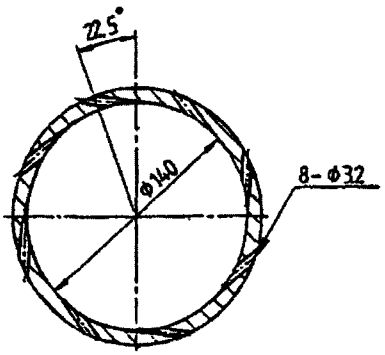

Fig. 3 Cross-section of the swirl generator

adjust the swirling intensity, the swirling generator was designed so that it could move in the swirl chamber. Fig. 2 shows the schematic arrangement of the test tube, swirl generator, and the multi-Pitot tube schematically.

3. Procedure for Heat Transfer Measurements

The manufacturer (Taurus Controls Ltd.) of the multi-Pitot tube certified it only for non-swirling, so before performing the test, it had to be calibrated for non-swirling flow of Re=10000~95000 and for swirling flow of Re=15000~80000.

The thermocouple used in this experiment was a K-type thermocouple with a diameter of 0.5 mm. After finding the average velocity and exit pressure of air to experiment on the calibration curve chart of the multi-Pitot tube, the air pressure was raised to a specified pressure by adjusting the rpm of the turbo fan motor suction the indoor air. In the air pressure equilibrium state, electric power (240 V, 2.6 kW) was supplied to the heating coil, and then the temperatures of the wall and local fluid in thermal equilibrium were measured and recorded by the thermocouples and the temperature recorder. The temperature recorder (Yokogawa, Model HR 2300) recorded the wall and fluid temperature at 2 minute intervals. The experiments continued until the temperature stopped changing. Equilibrium state of the fluid could be attained after about 30 minutes after the test began. Thermocouples were installed

in 14 locations at X/D=0.5, 1, 1.5, 2, 3, 4.5, 8, 12, 16, 20, 24, 28, 29, 29.5, and the wall and local fluid temperatures were measured at these locations.

The wall temperatures were decided as an arithmetic mean temperature because 4 thermocouples in a section were installed at 90° intervals of the circumference. The local fluid temperatures were measured at 1 mm intervals by the thermocouple feed mechanism. In this case, there were 14 measurement locations; they were measured in the same way as the wall temperatures were. The non-swirling flow temperatures were measured according to the Reynolds number, but for the swirling flow, Reynolds number and the swirl intensity, L/D were used.

4. Experimental Results and Discussion

4.1 Static pressure distributions

The static pressures for Re=40000 to 75000 at the 14 locations X/D=0.5, 0.8, 1.5, 2.0, 4.0, 5.0, 6.1, 7.3, 8.0, 10.2, 14, 18, 24, 26.5 were measured at the concave and convex tube by inclined Manometer (Air flow, MK5) before performing the heat transfer experiment.

Furthermore, 14 numbers of 2 mm static pressure holes were drilled into the concave tube. Then, 2 mm tubes were installed and connected to the Manometer, which could measure the static pressure of the fluid. Two mm static pressure holes were pierced and one end of the 2 mm copper tubes was connected to the inclined manometer, and the static pressure of air was measured.

At this moment, y-direction locations between the concave and convex tubes were being prepared to be precisely coincide with a transmitter so that the experiment could be performed.

Figure 4 and Fig. 5 show the static pressures of the fluid for Re=40000~75000, which was flown through the concave and convex tubes. The static pressure of the wall was high at the test tube entrance, but gradually decreased along the tubes (increased in the Fig. 4 and Fig. 5). This appeared to be high at the test tube entrance by

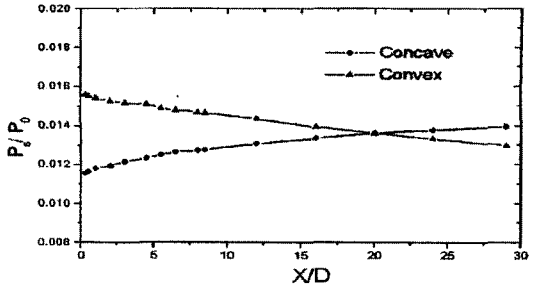

Fig. 4 Distributions of the static pressure along the test tube with swirl for Re=40000

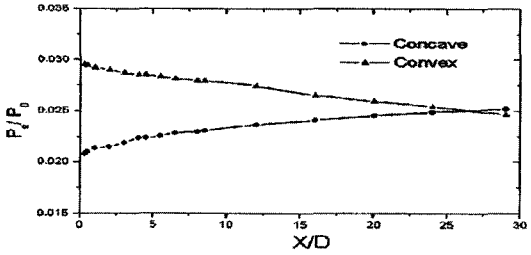

Fig. 5 Distributions of the static pressure along the test tube with swirl for Re=75000

the tangential velocity component of the swirling flow, and the static pressure also increased. This static pressure gradually decreased as the swirling flow decreased along the tube.

But for the convex tube wall, the static pressure was low at the tube entrance but gradually increased along the tube (decreased in Figure).

Near the tube entrance, the negative velocity zone usually formed in the direction of the convex wall due to the swirl intensity. It was unusual that there was a cross point of two static pressures (as they were swirl-decayed). In Re=40000, it was at about at X/D=20, but in Re=75000, it was at about X/D=27. This result implied that when the Reynolds number increases, the point moves away from the entrance of the annuli. This was thought to have come from that the swirl intensity was a function of the Reynolds number.

4.2 Friction factor

Using equation (1), the tube friction factor of the swirl and non-swirl flow was drived. In the fully developed zone, the friction coefficient was applied as the Blasius' equation.

$$f=\frac{\tau_w}{0.5\rho U^2} \quad (1)$$

The friction factors of the concave and convex tubes, respectively, were calculated from information in the static pressure distribution chart of Figs. 3 and 4. Figure 5 compares the friction factor (f_s) of the swirl flow for Re=40000 in the concave tube with that derived for the horizontal short tube by Sparrow et al.(1984).

In the annuli, fs/f of the concave tube was about 10 times higher than that of the non-swirling flow. It is likely that in the swirling flow, this result came from the tangential velocity component. The result was compared with that from the Sparrow's work (1984). His Reynolds number was 43500 with swirling flow of the horizontal single tube. The value in the entrance of the test tube was shown to be 1.7 times higher than that of the annuli, and in the end of the tube it was 6.3 times higher. The comparison of the f_s/f of the annuli for Re=75000 with that of Medwell et al. (1989) are given in Fig. 7. Medwell's results also appeared to be about 2 times higher in the tube entrance and 5.2 times higher in the tube end than in the annuli. As it were, the f_s/f in the swirling flow was shown to be 1.7~2.0 times higher in the test tube entrance and 5.2~6.3 higher in the tube end than in the annuli. This phenomenon is thought to have occurred due to the swirling flow in the annuli to accelerate the nullification of the swirling flow from the friction of the concave and the convex tube. The friction coefficient of the concave and convex tube along the test tube are given for the Reynolds number 40000, as shown in Fig. 8 and 9.

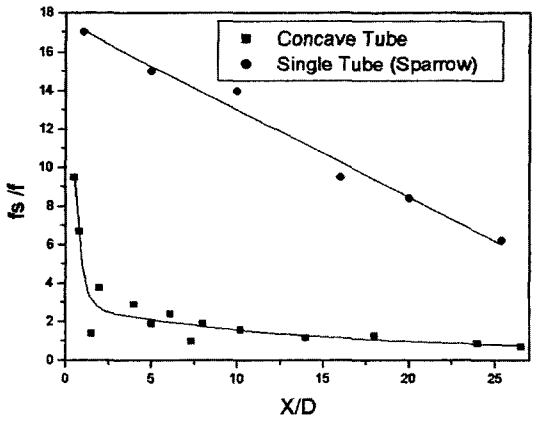

Fig. 6 Comparisons of the friction factor on the concave tube and the single tube with swirl for Re=40000

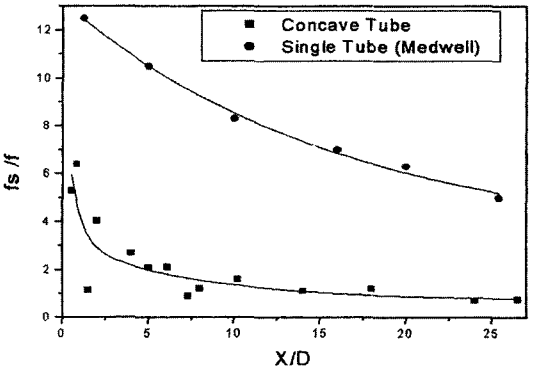

Fig. 7 Comparisons of the friction factor along the test tube with swirl for Re=75000

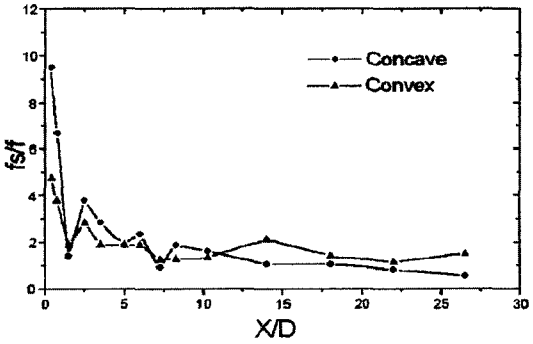

Fig. 8 Distributions of the friction factor along the test tube with swirl for Re=40000

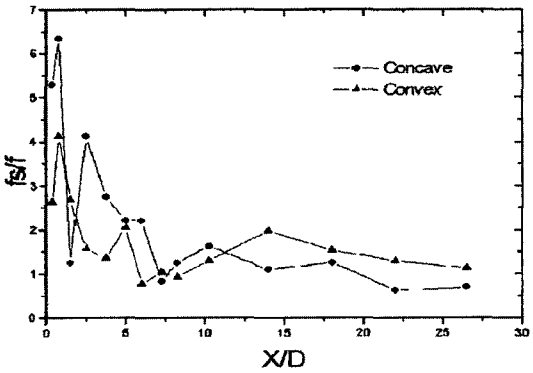

Fig. 9 Distributions of the friction factor along the test tube with swirl for Re=75000

In the tube entrance, f_s/f of the concave tube is shown to be about 9.6, but in the convex tube about 5.0. In Re=75000, it is 5.3 in the concave tube and 2.6 in the convex tube. In the convex tube, fs/f increased from 2.6 to 5.0 and then decreased, but in the concave tube, f_s/f increased from 5.3 to 9.6 and then decreased along the test tube. When the Reynolds number increased, a flow reversal zone near the convex tube enlarged. Therefore, this caused fs/f to decrease. Furthermore, these tube friction coefficients had their result cross each other. Namely, they crossed at X/D=10.5 in Re=40000 and X/D=11.0 in the 75000. These results were considered as recirculating zones appearing at the test tube entrance when having a strong swirling flow like the static pressure distribution.

4.3 Local air temperature distributions

Figure 10~Fig. 12 include the local fluid temperature (T/T_r) of the non-swirling flow at Re=30000, 50000 and 70000 respectively. For the non-swirling flow, the air temperature at Re=30000 was consistent when X/D=0.5~4.5, $y/(R_o-R_i)=0.7$, but as X/D increased, T/T_r gradually increased. Near the concave tube wall, the air temperature sharply increased and appeared to increase further as the Reynolds number decreased. Meanwhile the local temperature distribution of Re=30000 near the convex tube was 1.0~2.3 at $y/(R_o-R_i)=0.325$ but smaller when the Reynolds number increased, and at Re= 70000, the local temperature distribution appeared as $y/(R_o-R_i)=1.1\sim1.7$. It was thought that as the Reynolds number decreased, the temperature distribution near the convex tube would vary, but as the Reynolds number increased, the temperature distribution decreased due to the axial velocity increment. The fluid temperature decreased, regardless of the change of the Reynolds number. But, the dimensionless temperature (T/T_r) was decreased at X/D=29.0~29.5, with no relation with the change of the Reynolds number. The effect of the tube end may have decreased T/T_r. This phenomenon also appeared to have no relation with the change of Reynolds number.

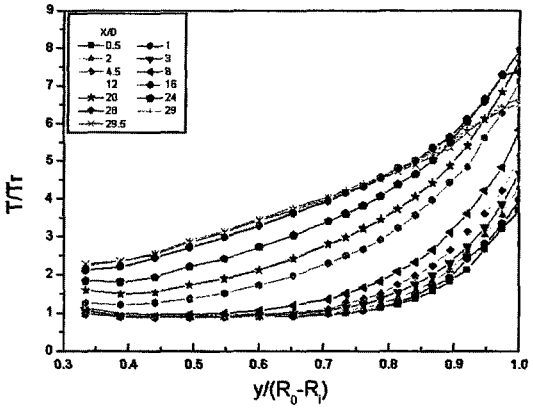

Fig. 10 Distributions of Tempeture Profile without Swirl across the Test Tube for Re=30000

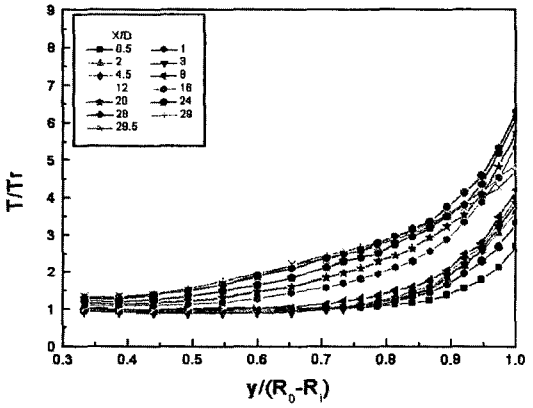

Fig. 11 Distributions of Tempeture Profile without Swirl across the Test Tube for Re=50000

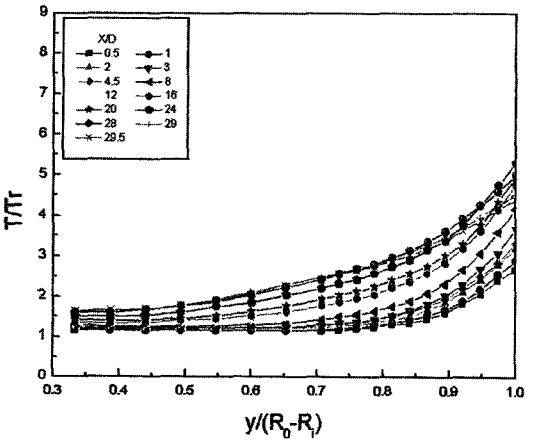

Fig. 12 Distributions of Tempeture Profile without Swirl across the Test Tube for Re=70000

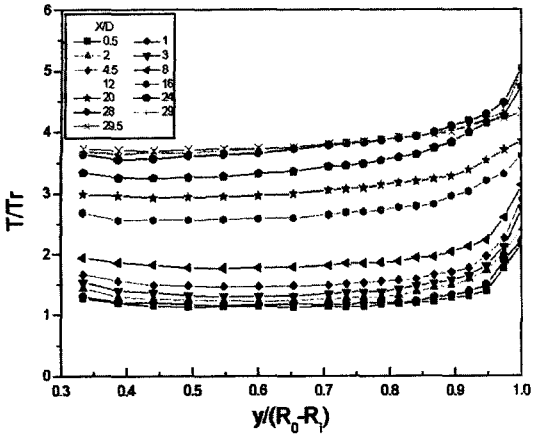

Fig. 13 Distributions of Tempeture Profiles with Swirl across the Test Tube for Re=30000

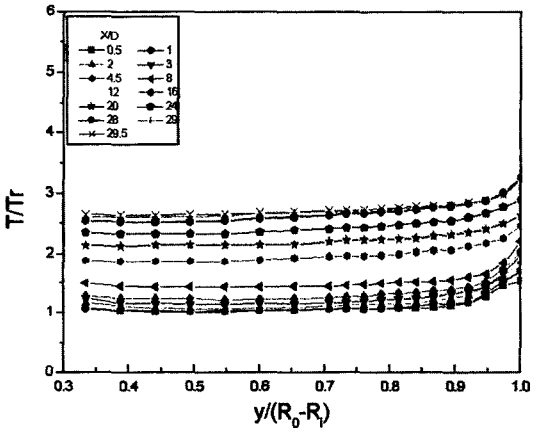

Fig. 14 Distributions of Tempeture Profiles with Swirl across the Test Tube for Re=50000

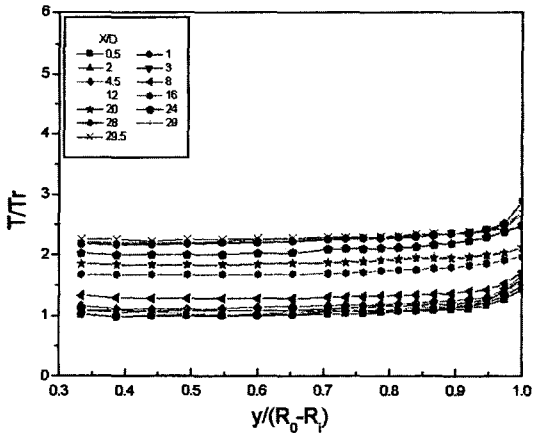

Fig. 15 Distributions of Tempeture Profiles with Swirl across the Test Tube for Re=70000

Figure 13~Fig. 15 show the local fluid temperature (T/T_r) of the air with swirling flow, and it appears to be consistent to $y/(R_o-R_i)=0.325\sim0.9$ for Re=30000 but the local fluid temperature is different that of the non-swirling flow. Except for the near tube wall, the temperature in the y-direction of the test tube appeared to be consistent even though X/D increased.

The temperature gradient near the tube wall sharply increased in the small range compared with non-swirling flow. The tangential velocity component of the swirling flow was regarded to transfer more energy from the tube wall to the fluid than that of the non-swirl flow. In addition, when the Reynolds number increased, the local temperature near the convex tube decreased, and the temperature range apparently decreased compared with non-swirling flow so that at Re=30000, the range was 1.2~3.65 at $y/(R_o-R_i)=0.325$ but at Re=70000, 1,0~2.3. The energy from the heated wall was transferred to the near convex tube wall with the fluid mixture because of the tangential velocity of the swirl flow. At the end of test tube, the effect of the tube end appeared to be similar to that of the non-swirling flow, but the range of the temperature gradient was smaller than that of the non-swirling flow.

4.4 Wall temperature and dimensionless Temperature

Figure 16 depicts the relation between the Reynolds number and the wall temperature (T_w/T_r) of the non-swirling flow. At the tube entrance the wall temperature distribution sharply increases, but after X/D=10, and up to 24 it gradually increases. Namely, this range is regarded as the thermally full developed region in the annuli, but after X/D=25, this region decreases along the test tube. This temperature distribution in such phenomena is the same as the local fluid temperature distribution of the tube end regarded as the effect of the tube end. The wall temperature distribution decreased as the Reynolds number increased, this decrease means that as more energy from the wall was transferred to the fluid, the average velocity increased according to the Reynolds number.

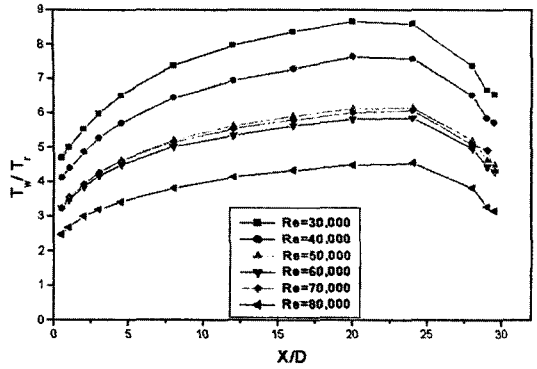

Fig. 16 Comparison of T_w/T_r without swirl for Re=30000, 40000, 50000, 60000, 70000 and 80000

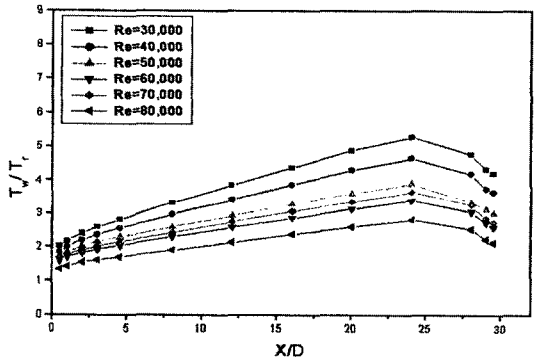

Fig. 17 Comparison of T_w/T_r with swirl for Re=30000, 40000, 50000, 60000, 70000 and 80000

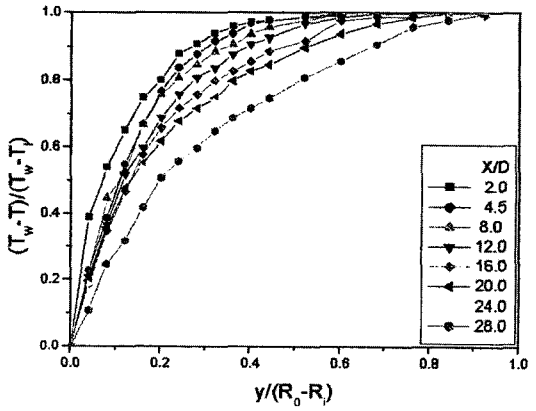

Fig. 18 Distributions of $(T_w/T)/(T_w/T_i)$ without swirl for Re=50000

Figure 17 also includes the wall temperature in the swirling flow. T_w/T_r of the test tube entrance, which was 2.5~4.6 in the non-swirling flow, was much lower in the swirling flow, 1.3~2.0. Furthermore, the maximum temperature, which was 8.8 in the non-swirling flow, was very low, 5.2, in the swirling flow. This low number means that the swirl flow transferred more energy from the heated tube wall to the fluid than the non-swirling flow did. But this phenomenon is consistent with the local fluid temperature variation.

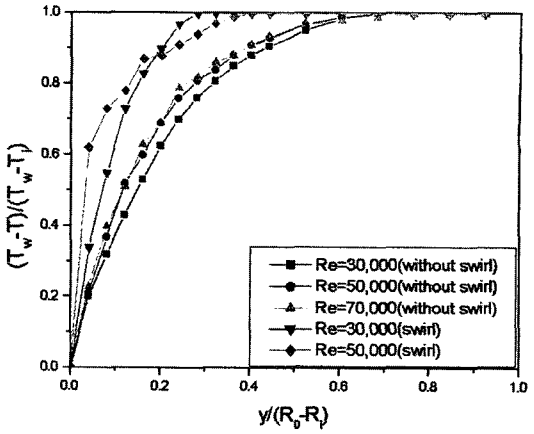

Fig. 19 Comparisons of $(T_w/T)/(T_w/T_i)$ with swirl and without swirl at X/D=12

Figure 18 shows the radial dimensionless temperature distributions $(T_w/T)/(T_w/T_i)$ for non-swirl flow. Here, wall and local air temperatures have been taken from earlier plot.

This diagram serves to emphasize the main feature of a developing thermal boundary layer. Figure 19 shows the comparisons of the dimensionless temperature distributions of swirl and without swirl flow at X/D=12. The 'squareness' of the temperature profiles of swirl flow is more 'flat' than that of non-swirl flow.

4.5 Comparisons of nusselt number with swirl and without swirl flow

The fundamental bulk temperature could be calculated from equation (2), but because it was found out after measuring the local fluid temperature and the axial velocity, the bulk temperature of each zone was calculated by equation (3), and the local Nusselts number was done by equations (4), (5) and (6). Finding out the bulk temperature from the local fluid temperatures of Fig.

10~Fig. 15, and the specific heat and heat transfer coefficient of the fluid, Nusselt number was calculated for swirl flow and non-swirl.

$$T_b=\frac{\int_0^{r_0} 2\pi\rho\, dr\, uc_pT}{\int_0^{r_0} 2\pi\rho\, dr\, uc_p} \tag{2}$$

$$T_b=\frac{1}{A}\int_A TdA \tag{3}$$

$$dq=mc_pd\ T_b \tag{4}$$

$$h=\frac{mc_pd\ T_b}{2\pi r\ dx(T_w-T_b)_{mean}} \tag{5}$$

$$Nu=hD/k \tag{6}$$

The calculated Nusselts number was compared with the results, which were calculated from the Dittus & Boelter equation. Here, Pr is the Prandtl number.

$$Nu_d=0.0023Re^{0.8}\mathrm{Pr}^{0.4} \tag{7}$$

Detailed Nusselt number distributions are given for Re=30000~80000 for without swirl flow in Fig. 20. In this result, Nu_s/Nu_d at the tube entrance was 1.5~1.7, but at the exit, 1.4~2.05. Nu_s/Nu_d of the tube entrance gradually decreased along the test tube. The thermally full developed region was initiated and maintained from about X/D=10 to 22.25 and then increased again at the end of the tube. This behavior continued regardless of the Reynolds Number. When the air flew along the test tube, and this air flow was heated, thus, the region increased. Moreover, in the fully developed region, the Nusselt number was shown to be lower than that of Dittus & Boelter equation. This difference was probably due to the heat loss in the convex tube.

Figure 21 shows the dimensionless Nusselts number (Nu_s/Nu_d) of the swirling flow according to the Reynolds Number. The Nusselts number for the swirling flow changed according to Reynolds number, and was influenced by the effects at the tube entrance, and exit. At the entrance, Nu_s/Nu_d was 3.6~5, and at the exit, to be higher than 4.5~6.

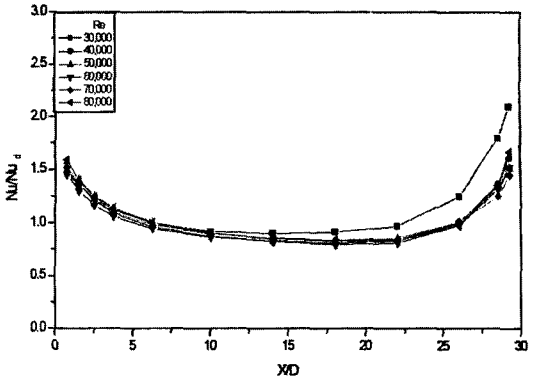

Fig. 20 Comparison of Nussults Number without Swirling Flow for Re=30000, 40000, 50000, 60000, 70000 and 80000

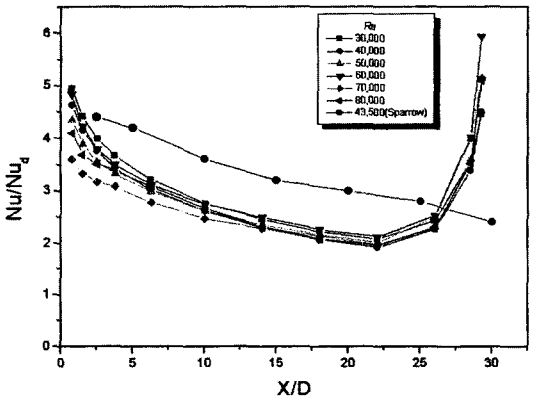

Fig. 21 Comparison of Nussults Number with Swirl for Re=30000, 40000, 50000, 60000, 70000 and 80000

A particular phenomenon was that in the swirling flow there was no fully developed region. This result coincides with investigation results that have been so far published in the single horizontal tube.

This figure includes comparison with the results of Sparrow et al.(1984). He employed an Ohmic heating method to utilize the electric resistance of the tube material itself, which was made of a single piece of stainless steel. Nusselts number at the entrance was almost the same but gradually decreased and at the end of the tube, decreased to 2. 41 without the effect of the tube end.

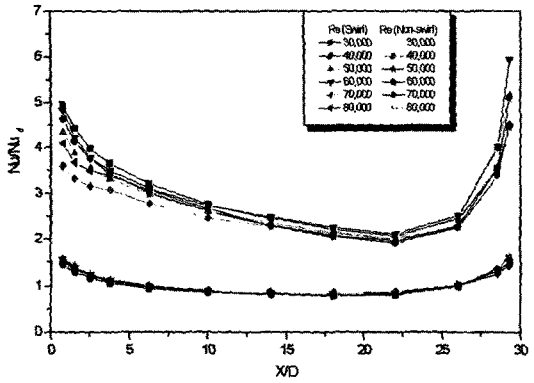

Fig. 22 Comparison of Nusselts number with Swirl and without swirl for Re=30000, 40000, 50000, 60000, 70000 and 80000

Figure 22 also includes the comparisons between Nusselts number over the Reynolds number range of Re=30000~80000 with swirling and without swirling flow. Nusslts number of swirling flow was observed to be 2.0~2.5 times bigger than the one for the non-swirling flow at X/D= 10~25. It also was observed to be 2.3~3.3 times bigger at the tube entrance and 3~4 times bigger at the end of the tube. It is thought that the swirling flow could transfer more heat by fluid mixing due to tangential velocity.

It means that the Reynolds Number is a function of swirl intensity. If the Reynolds Number is increased, the tangential velocity is increased and the heat transfer from the heated wall is also increased.

5. Conclusions

The following conclusion were derived from heat transfer experiments where the swirling and non-swirling flow moved through a horizontal annuli of air fluid.

(1) There was a region where the static pressure and the tube friction factor could cross in the concave and the convex tube.

(2) The friction factor in the concave tube of the annuli was 1.7~2.0 times lower at the tube entrance and 5.2~6.3 times lower at the exit than that of the single test tube.

(3) The fluid temperature distribution from the convex to concave tube in the swirling flow was consistent up to $y/(R_o-R_i)=0.9$. This phenomenon continued as the Reynolds number increased.

(4) The Nusselts number of the swirling flow was observed to be 2.0~2.5 times higher than one in the fully developed regions of the non-swirling flow. It was regarded as a phenomenon that owing to the tangential velocity component of the fluid, caused more energy to be transferred from the heated wall in the swirling flow to the fluid than in the non-swirl flow.

(5) In the fully developed zone without swirl flow, the Nusselt number was lower than that of Dittus & Boelter equation. However, the swirling flow has no fully developed region.

Acknowledgments

This work is supported by Kyungnam University research fund, 2003.

References

Rothfus, R. R., 1948, Velocity Distribution and Fluid Friction in Concentric Annuli, Ph. D. thesis, Carnegie Institute of Technology.

Brighton, J. A. and Jones, J. B., 1964, "Fully Developed Turbulent Flow in Annuli," *J. of Basic Engineering*, pp. 835~843.

Alan, Q., 1967, "An Experimental Study of Turbulent Flow Through Concentric Annuli," *Int. J. Mech. Si*, Vol. 9, pp. 205~221.

Kay, W. M. and Leung, E. Y., 1963, "Heat Transfer in Annular Passages : Hydro dynamically Developed Flow with Arbitrarily Prescribed Heat Flux," *Int. J. Heat Mass Transfer*, Vol. 6, pp. 537~557.

Tuft, D. B. and Brandt, H., 1990, "Forced Convection Heat Transfer in a Spherical Annulus Heat Exchange," *J. of Heat Transfer*, Vol. 104, pp. 670~677.

Molki, M., Astill, K. N. and Leal, E., 1990, "Convective Heat-mass Transfer in Temperature Region of a Concentric Annulus having a Rotating inner Cylinder," *Int. J. Heat and Fluid Flow*, Vol. 11, No. 2.

Garimella, S. and Chritensen, R. N., 1995, "Heat Transfer and Pressure Drop Characteristics of Spirally Flute Annulli : Part II Heat Transfer," *J. of Heat*, Vol. 117, pp. 55~68.

Chigier, A. N. and Beer, J. M., 1964, "Velocity and Static Pressure Distributions in Swirling Air Jets Issuing From Annular and Divergent Nozzle," *ASME, J. of Basic Engineering*, pp. 788~796.

Scott, C. J. and Raske, D. R., 1973, "Turbulent Viscosities for Swirling Flow in a Stationary Annulus," *ASME J. of Fluid Engineering*, pp. 557~566.

Milar, D. A., 1979, "A Calculation of Laminar and Turbulent Swirling Flows in Cylindrical Annuli," ASME, Winter Annual Meeting New York Dec. pp. 89~98.

Clayton, B. R., and Morsi, Y. S. M., 1985, "Determination of Principal Characteristics of Turbulent Swirling Flow Along Annuli," *Int. J. Heat & Fluid Flow*, Vol. 6, No. 1, pp. 31~41.

Reddy, P. M., Kind, R. J. and Sjolander, S. A., 1987, "Computation of Turbulent Swirling Flow in an Annular Duct," Num.. Method in Laminar and Turbulent Flow, pp. 470~481.

Chang, T. H. and Kim, H. Y., 2001, "An Investigation of Swirling Flow in a Cylindrical Tube," *KSME Int. J.*, Vol. 15, No. 12, pp. 1892~1899.

Ahan, S. W., Lee, Y. P. and Kim, K. C., 1993, "Turbulent Fluid Flow and Heat Transfer in a Concentric Annuli with Square-Ribbed Surface Roughness," *J. of KSME(B)*, Vol. 17, No. 5, pp. 1297~1303.

Kim, K. C., Ahan, S. W. and Lee, B. G., 1994, "Turbulent Structure in Flow in Concentric Annuli with Rough Outer Wall," *J. of KSME (B)*, Vol. 18, No. 9, pp. 2443~2453.

Kim, K. C., Ahan, S. W. and Jung, Y. B., 1995 "Effect of Surface Roughness on Turbulent Concentric Annular Flows," *J. of KSME(B)*, Vol. 19, No. 7, pp. 1749~1757.

Ahan, S. W., 1999, "Friction Factors for Flow in Concentric Annuli with Roughened Wall," *J. of KSME(B)*, Vol. 23, No. 5, pp. 587~592.

Sparrow, E. M. and Chaboki, A., 1984, "Swirl-Affected Turbulent Fluid Flow and Heat in a Circular Tube," J. of Heat Transfer ASME, Vol. 106, pp. 766~773.

Medwell, J. O., Chang, T. H. and Kwon, S. S., 1989, "A Study of Swirling Flow in a Cylindrical Tube," Korean J. of Air-Conditioning and Refrigeration Engineering, Vol. 1, pp. 265~274.